Observation of Diffusion and Tunneling Recombination of Dye-Photoinjected Electrons in Ultrathin TiO_2 Layers by Surface Photovoltage Transients

Iván Mora-Seró,*,† Thomas Dittrich,‡ Abdelhak Belaidi,‡ Germà Garcia-Belmonte,† and Juan Bisquert*,†

Departament de Ciències Experimentals, Universitat Jaume I, E-12080 Castelló, Spain, and Hahn-Meitner Institut, Glienicker Strasse 100, 14109 Berlin, Germany

Received: April 15, 2005; In Final Form: May 31, 2005

Surface photovoltage transients were used to monitor both the short time dynamics (>10 ns) and the spatial distribution of electrons photoinjected in thin (2−20 nm) TiO_2 layers from dye molecules adsorbed at the surface. At low temperatures (100−250 K), the dynamics are governed exclusively by spatially dependent tunneling recombination, with a rate that varies with the distance from the surface x as $\exp(-2x/a)$, and an initial exponential distribution of photoinjected electrons, $n_0 \exp(-x/b)$. This model is confirmed by the observation of power law decay in time $t^{-a/2b}$ with a ratio $a/b = 0.28 \pm 0.04$. The stability of *cis*-di-(isothiocyanato)-*N*-bis(2,2′-bipyridine-4,4′-dicarboxy) ruthenium(II) (N3) dye molecules on TiO_2 during treatment in a vacuum at high temperatures was proven. For high temperatures (250−540 K), the thickness dependence of the decays indicates that the dynamics of surface recombination are retarded by the diffusion of electrons toward the interior of the film. The implications for thin layer coating in dye-sensitized solar cells are discussed.

1. Introduction

Electronic processes in TiO_2 nanoporous films have been amply investigated in relation with dye-sensitized solar cells (DSSCs).[1] It is well-known that the operation of DSSCs relies on a competition of electron extraction by diffusion over the whole TiO_2 nanoporous film (typically 10 μm thick) and recombination in the huge internal surface both with redox species in solution and oxidized dye molecules. Several authors[2−4] have suggested that the rate of recombination is influenced by the rapidity of transport at the microscopic level, since the latter factor determines the chance for an electron to hit a recombination site in the nanoparticle surface. However, a separate investigation of transport and recombination at very short temporal and spatial scales in DSSCs poses some difficulties. Techniques operating in the intermediate time/frequency range (10 mHz to 1000 Hz) such as impedance spectroscopy,[5] transient photocurrents,[4] and open-circuit photovoltage decays[6] provide macroscopic parameters that are time- and spatial-averaged with respect to the microscopic processes.[7] The latter are resolved separately in fast optical pump−probe experiments (10 ns to 10 ms), for example, monitoring the decay of the photoinduced dye cation excited by a laser pulse.[2] However, direct information about spatial distribution of carriers cannot be obtained from an optical measurement itself.

Ultrathin TiO_2 layers can serve as a model system to investigate the coupling of intraparticle transport with interfacial charge transfer, which may be useful for a better understanding of carrier transport and recombination in a network of interconnected nanoparticles.[8,9] In addition, ultrathin oxide layers have gained increasing relevance as effective coatings for improving the performance of DSSCs.[10−12] Very recently, Zaban and coworkers[13] analyzed a new type of high surface area TiO_2 electrode for DSSCs, consisting of a transparent conductive nanoporous matrix that is coated with a thin layer of TiO_2. This design ensures a several nanometer distance between the TiO_2−electrolyte interface and the current collector throughout the nanoporous electrode, in contrast to the several micron distance associated with the standard electrode. In that work,[13] they show that the photovoltaic performance (measured by open-circuit photovoltage) of TiO_2 coating thinner than 6 nm is rather inefficient. It was suggested that the region closer to the surface plays a special role in recombination so that very thin layers prevent electron accumulation.

In this work, we present an investigation of recombination and transport of photoinjected electrons in ultrathin TiO_2 layers by means of the dynamic method of surface photovoltage (SPV) transients.[14] These transients are measured in a vacuum in the capacitor arrangement.[15] As found in previous experiments and checked in this work by transmission measurements, *cis*-di-(isothiocyanato)-*N*-bis(2,2′-bipyridine-4,4′-dicarboxy) ruthenium-(II) (N3) dye molecules adsorbed at TiO_2 are stable in a high vacuum even at high temperatures,[16] and measurements for different temperatures between −170 and 270 °C have been achieved. SPV measurements give information both about time scales below 10 ns and length scales of charge separation over very short distances on the order of nanometers. Therefore, we are able to investigate in detail the spatial distribution of electrons in the thin layer and its evolution with time. It has been shown[17] that recombination to oxidized dye molecules is a tunneling reaction, the rate of which depends strongly on the distance between the TiO_2 surface and the metal center of the dye. Our results at low temperatures will provide information on the initial distribution and tunneling parameters of this process.

* Authors to whom correspondence should be addressed. E-mail: Bisquert@uji.es. E-mail: Sero@uji.es.
† Universitat Jaume I.
‡ Hahn-Meitner Institut.

10.1021/jp058128w CCC: $30.25
Published on Web 07/14/2005

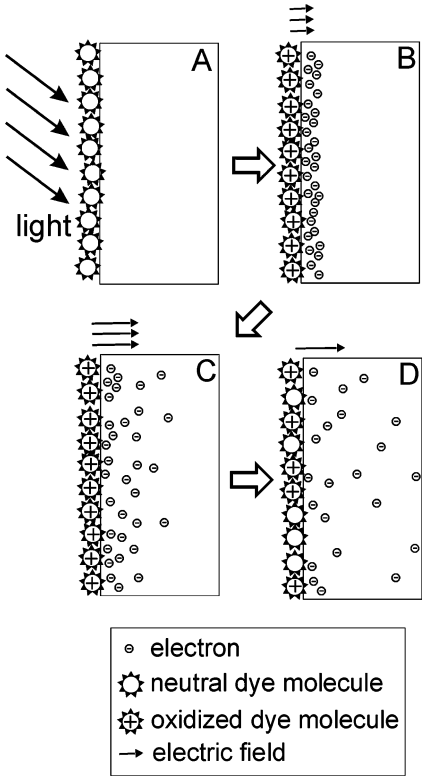

Figure 1. Scheme of elementary processes in the investigated model system consisting of a thin TiO_2 layer sensitized with dye molecules at the surface. The photovoltage is given by the amount of separated charge and by the effective charge separation length. (A) Laser excitation. (B) Initial charge separation. (C) Diffusion. (D) Recombination.

Figure 1 gives an overall view of the various possible processes that contribute to the spectral shape of SPV in a temporal sequence. At each moment, the measured PV corresponds to the electrical field due to the spatial separation of electron and oxidized dye molecules. First, the laser produces electronic excitation in the dye (A). Electrons are injected from the photoexcited dye into the TiO_2 layer, leaving an uncompensated positive charge in the dye (B). This charge separation process may proceed within tens of femtoseconds during ultrafast injection from dye molecules into TiO_2 and produces an initial distribution of electrons close to the surface and the starting SPV signal. Subsequently, electron diffusion increases the extent of charge separation and consequently the SPV signal (C).[8,9] Back electron transfer to the oxidized dye molecules (recombination) decreases the amount of free electrons and consequently the SPV. In zero-current measurement conditions, the back contact behaves as a blocking interface, limiting the extent of spatial charge separation (D). Experimentally, these steps occur sequentially or simultaneously; for example, the final stages of the decay may be dominated by a diffusion-limited supply of electrons to the region within a tunneling distance of the dyed surface. An interpretation of the experimental results based on a physical model will be presented below.

2. Experimental Section

Compact ultrathin TiO_2 layers were prepared on conducting SnO_2/F substrates by the so-called ion layer gas reaction (ILGAR) technique.[18] For the ILGAR treatment, a robot was used. During the ILGAR procedure, the sample is subsequently dipped in a precursor salt solution (0.03 M $TiCl_4$ in tetrahydrofuran (THF)), oxidized in a gaseous stream of aqueous NH_3 (it contains NH_4^+ and OH^-) at 400 °C for 45 s, cooled in a N_2 stream for 40 s, rinsed in H_2O, and dried in THF. The thickness of the TiO_2 layer was adjusted by repeating the complete ILGAR procedure while one cycle corresponds to one dip in the precursor salt solution. The related thickness of a deposited compact metal oxide layer is 1−2 nm/dip (see also ref 19 for details). The amount of deposited Ti atoms in the TiO_2 layers was determined by elastic recoil detection analysis (ERDA); for details, see also ref 19. With respect to this analysis, the thicknesses of the compact TiO_2 layers were about 2, 4, and 20 nm (1, 3, and 10 dips, respectively). It has been checked by Raman spectroscopy that thicker TiO_2 layers consist of anatase and amorphous phases after annealing at 400 °C. Additionally, to show the effects of diffusion, a compact TiO_2 layer (100 nm thick) has been prepared by spray pyrolysis on a hot substrate (ECN); for details, see ref 20 and references therein.

TiO_2 layers and a bare substrate were sensitized with the N3 dye by dipping in a 0.5 M dye solution for 20 s. SPV transients were measured in the capacitor arrangement[15] with a thin mica layer as spacer. A 10 GΩ load resistor, a high-impedance 500 MHz buffer (input resistance >100 GΩ, output resistance 50 Ω), and a 300 MHz sampling oscilloscope were used for the transient measurements with a resolution time of the whole system better than 2 ns. The *RC* time constant of the measurement circuit, i.e., sample with load resistor, was about 0.3 s. The SPV transients were excited below the TiO_2 band gap with pulses of the second harmonic of a Nd:YAG laser (duration time 120 ps, wavelength 532 nm, excitation intensity at the sample $I_0 = 0.3$ mJ/cm^2). The repetition rate of the laser pulses was 1 Hz for all measurement. The samples were deposited into a homemade cryostat (pressure 10^{-6} mbar), allowing temperature-dependent SPV measurements between −170° and 270 °C. To analyze the possible contribution of the charge trapping on SnO_2 surface states, measurements on bare substrate sensitized with the N3 dye also have been carried out.

The stability of N3 dye molecules on TiO_2 during treatment in a vacuum at high temperatures was proven by using nanoporous TiO_2 layers dyed with N3 molecules overnight so that the transmission dropped to about 1%. The optical transmittance spectra were measured with a quartz prism monochromator, a halogen lamp, and a Si photodiode as a detector. The spectra were normalized to the untreated TiO_2 while scattering and changes in scattering were not taken into account.

Figure 2 shows the transmittance spectra after heat treatment in air (a) and vacuum (b). The transmission of the dyed TiO_2 is around 1.6 eV, and it is characterized by a minimum around 2.2 eV. The transmission spectra change dramatically, and the transmission increases strongly after heat treatment in air due to the oxidation of dye molecules. In contrast, the characteristic transmission of the dyed TiO_2 is preserved after heating in a vacuum at 200 or 300 °C while the minimum was slightly blue-shifted and the transmission increased by about 7% and 40% in comparison to the untreated sample, respectively. The slight blue shift is probably induced by an increase in the number of bonding sites between the TiO_2 surface and the four hydroxyl groups per dye molecule at increased temperatures. The significant decrease of about 40% at 300 °C is caused by an increase in the decomposition rate of N3 dye molecules at high temperatures, probably due to an increase in the catalytic activity of TiO_2 by thermal generation of holes.

It is well-known that optically active defects are forming in TiO_2 under vacuum conditions. This can be seen in Figure 2b as a decrease in the transmission toward higher photon energies.

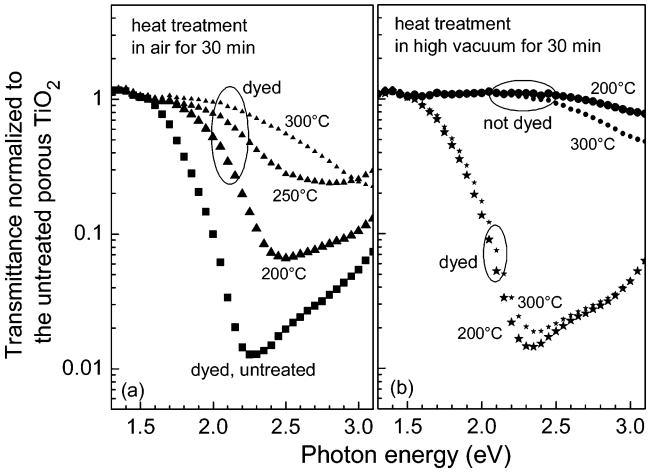

Figure 2. Transmittance spectra normalized to the untreated porous TiO_2 (anatase) for porous TiO_2 with adsorbed dye molecules after heating in air (a) or a vacuum (b). For comparison, the spectra are also shown for the bare TiO_2 after heating in a vacuum. The measurements are carried out in air at room temperature.

The defect generation became already significant at 300 °C. However, no remarkable change in the transmission was observed around 2.33 eV (second harmonic of the Nd:YAG laser) for the TiO_2 after heating in a vacuum even at 300 °C.

3. Results and Discussion

Figure 3 shows typical SPV transients for ultrathin dye-sensitized TiO_2 at different temperatures. The spectra are normalized to the SPV value at the resolution time of the system that coincides with the maximum recorded value. The signal and the maximum of SPV appear within the duration of the illumination pulse. At low temperature ($T \leq -20$ °C), the curves of the transients remain practically unchanged; while at higher temperatures, there is a delay in the SPV transients, producing a nearly plateau region followed by a fast decay. Figure 4 shows the SPV transients for ultrathin dye-sensitized TiO_2 layers of three different thickness and for a bare substrate at different temperatures.

All of the decays for samples with a thin layer of TiO_2 show long tails that extend into the second time scale. The SPV transient for low temperatures, Figure 4a, is independent of the film thickness. However, at high temperatures as the layer thickness increases, the retardation of the SPV becomes much larger, providing the plateau region for the thickest sample.

These observations can be explained in the following way. As indicated above, in Figure 1, first the electrons are injected in a narrow region of the TiO_2 layer in the dye/TiO_2 interface. Thereafter, the electrons may either recombine with the photooxidized dye molecules or diffuse away from the interface.

A different possible interpretation of the SPV observed in very thin layers is a fast charge trapping on SnO_2 (substrate) surface states immediately after photoinjection and later release by thermal emission over the barrier present at that interface. In this case, transit of electrons through the TiO_2 layer would not be detected. However, as can be observed from the results plotted in Figure 4, the dynamics of the decay in the bare substrate are faster than the dynamics observed for the samples with a thin layer of TiO_2; in this sense, it is not a limiting process, and its effect has not been considered in the model. In addition, measurements performed in much thicker samples of 100 nm, shown in Figure 5, display more clearly the diffusion process in terms of a photovoltage peak in the transient curve. (Note that the signal increase with time cannot be explained by a release from traps.) Furthermore, the results of Figure 4 show that the PV transients for the thin films depend on the film thickness as expected for a diffusion process and not from a dynamics controlled by the release from interfacial traps. It must be recognized that these arguments do not completelly rule out the possibility that if electrons arrive rapidly at the SnO_2 /TiO_2 interface, then they will transfer to the SnO_2 and there will be a significant thermal barrier to overcome to transfer back into the TiO_2 before recombination. However, the available evidence indicates strongly that the decays correspond to a diffusion dynamics, and this interpretation will be adopted below.

Hereafter, we first discuss the experimental results at low temperature, which are related to the recombination process, and then we consider the high-temperature results in which recombination is coupled with diffusion.

3.1. Low-Temperature Results. Since the low-temperature results are independent of layer thickness, one may assume that the initial distribution of injected electrons remains stationary in space and decays by recombination only. This is due to the fact that diffusion is a thermally activated process that is extremely slow at low temperatures and can be considered negligible. The low diffusion coefficient also implies a low mobility, and Coulomb interaction is neglected.

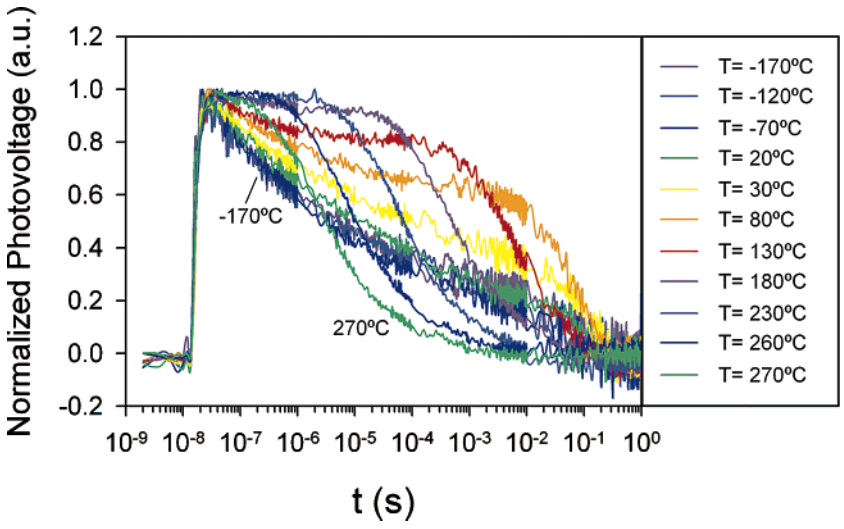

Figure 3. Normalized photovoltage spectra for a TiO_2 compact layer (10 dips) at different temperatures.

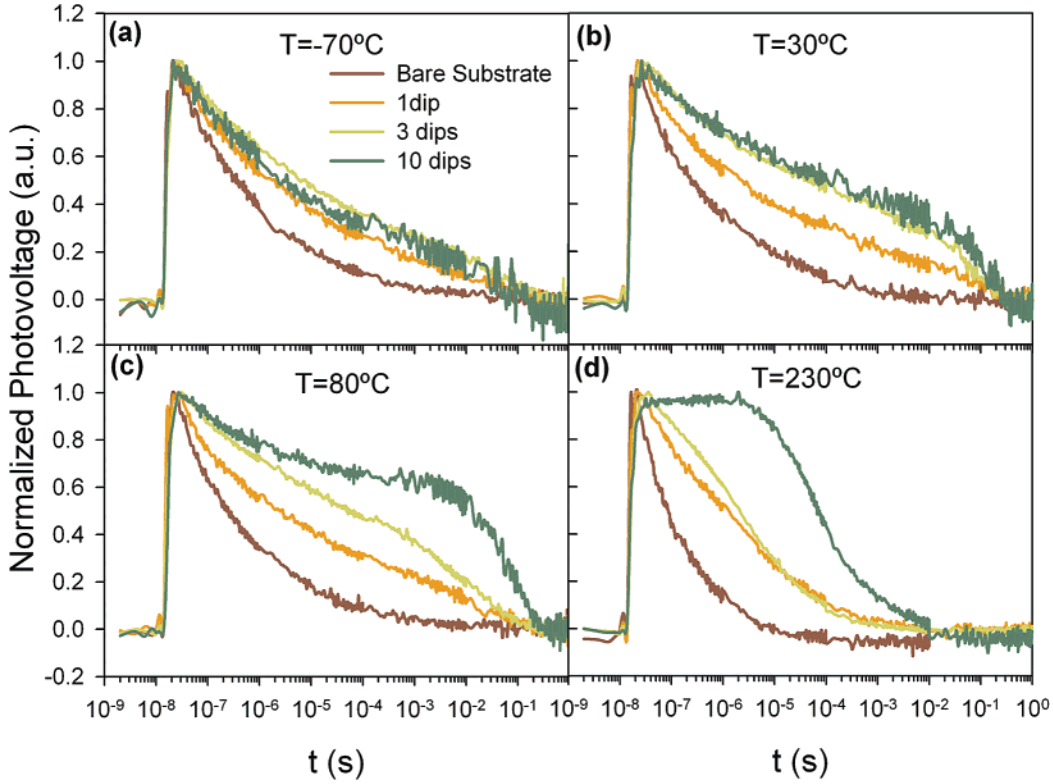

Figure 4. Normalized photovoltage spectra for TiO_2 compact layers with different thickness, 1−2 nm/dip, controlled by the number of dips (as indicated) employed in the ILGAR growth process.

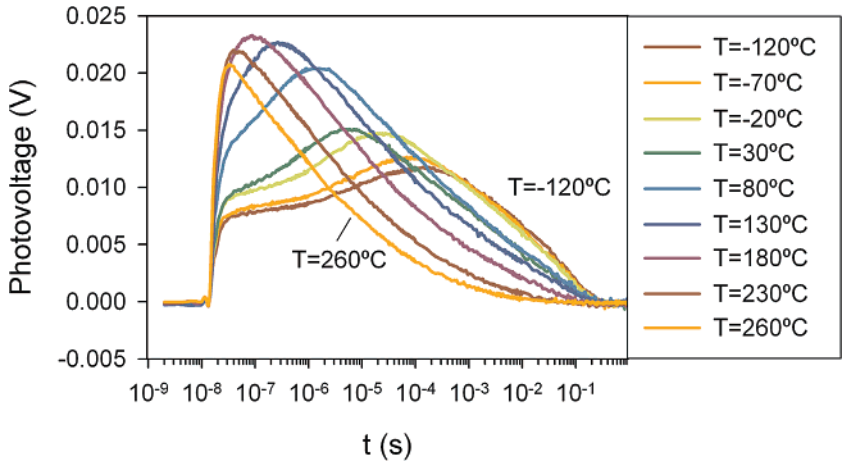

Figure 5. Photovoltage spectra for the TiO_2 compact layer of 100 nm in thickness at different temperatures.

The independence of the recombination process on the temperature implies that the recombination mechanism is not a thermally activated process. The spatially dependent tunnelling recombination meets this requirement. It is well-known as one mechanism for persistent photocurrents,[21] and it also has been employed to explain the SPV transients of ultrathin TiO_2 layers illuminated with a laser excitation above the TiO_2 band gap.[9] In the present scheme, the overlap of the wave functions of the electron, in the TiO_2, and the hole, in the dye, determines the recombination rate of spatially separated charge carriers.[17] The rate R of recombination of electrons at a distance x from the surface is

$$R(x) = \frac{\Delta n}{\tau_0} e^{-2x/a} \tag{1}$$

where τ_0 is a phenomenological parameter, the lifetime for vanishingly small spatial separation, and a is the electrons Bohr radius. The spatial distribution of excess electrons, $\Delta n(x,t)$, can be obtained from the equation

$$\frac{\partial \Delta n}{\partial t} = -\frac{\Delta n}{\tau_0} e^{-2x/a} \tag{2}$$

which can be solved exactly and yields the time-dependent electron distribution

$$\Delta n(x,t) = \Delta n_0(x) \exp\left[-\exp\left(-\frac{2x}{a}\right)\frac{t}{\tau_0}\right] \tag{3}$$

The exponential distance dependence of the tunneling phenomenon should lead to an exponential distribution immediately

after injection, considering that photoinjection of electrons from dyes into TiO_2 occurs also by tunneling.[22] A theory of geminate-ion recombination by tunneling from an initial exponential distribution was formulated by Tachiya and Mozumber,[22] predicting a time dependence t^{-m} for the integrated electron density. Here, we adopt a similar formulation for the calculation of the photovoltage in our system. We assume that the distribution of photoinjected electrons at the initial time, $\Delta n_0(x)$, with a number of electrons at $x = 0$ of n_0 is exponential with the width controlled by a b parameter. Hence

$$\Delta n(x,t) = n_0 \exp\left[-\frac{x}{b}\right] \exp\left[-\frac{t}{\tau_0}\exp\left(-\frac{2x}{a}\right)\right] \qquad (3)$$

The PV signal dependence on the electron distribution can be found by integrating the Poisson equation twice,[9] as follows

$$U(t) = \frac{e}{\epsilon\epsilon_0}\int_0^d dx \int_0^x \Delta n(y,t)\, dy \qquad (4)$$

where e is the elementary charge, $\epsilon_0 = 8.85 \times 10^{-14}$ F/cm, and ϵ is the dielectric constant of the layer; we have used a value of 50 for anatase TiO_2. Through the use of eq 3 in eq 4, $U(t)$ can be determined. If we define r as

$$r = \frac{t}{\tau_0}\exp\left(-\frac{2y}{a}\right) \qquad (5)$$

eq 4 can be expressed as

$$U(t) = \frac{en_0a}{2\epsilon\epsilon_0}\left(\frac{t}{\tau_0}\right) - \frac{a}{2b}\int_0^d dx\left(\Gamma\left(\frac{a}{2b}\right) - \Gamma\left(\frac{a}{2b},\frac{t}{\tau_0}\exp\left[-\frac{x}{2a}\right]\right)\right) \qquad (6)$$

where $\Gamma(p)$ is the gamma function and $\Gamma(p,Z)$ is the incomplete gamma function defined as follows

$$\Gamma(p,Z) = \int_Z^\infty \exp(-r)r^{p-1}\, dr \qquad (7)$$

For a sufficiently large Z, the incomplete gamma function tends to zero. In eq 6, this premise will occur when $t \gg \tau_0$, but the dependence of Z with x will introduce an error, even in the case when the condition $t \gg \tau_0$ is fulfilled, which we have estimated to be about 5%; see below. If this approximation is applied an analytic dependence of photovoltatge with time is obtained, as follows

$$U(t) = \frac{en_0ad}{2\epsilon\epsilon_0}\Gamma\left(\frac{a}{2b}\right)\left(\frac{t}{\tau_0}\right)^{-a/2b} \qquad (8)$$

the photovoltage obeys a time-dependent power law so that a straight line will be obtained in a log−log plot with a slope $-a/2b$.

Figure 6 shows the experimental value of SPV at low temperatures for different layer thicknesses and the SPV transients calculated from the model of eqs 3 and 8. For the three samples, straight lines are obtained with close slope values as the model predicts. It has been determined elsewhere[23] that the value $\tau_0 = 2$ ps is the shortest possible time for back charge transfer of an electron into a charged dye molecule in TiO_2. Figure 6 shows the results of calculations using two different values of a and b parameters. We find, averaging the slopes obtained for the three samples, that the ratio of the electron Bohr radius and the exponential parameter in the initial distribution, a/b, is 0.28 ± 0.04. In Figure 6, the SPV transients

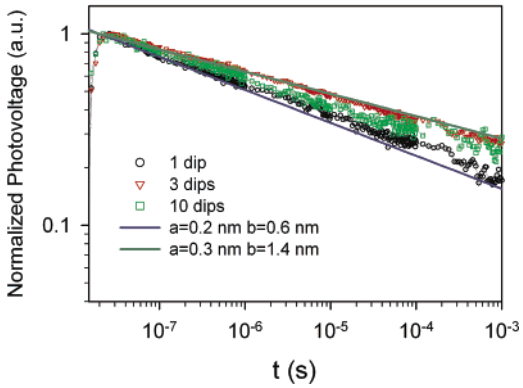

Figure 6. Comparison the normalized photovoltage spectra for TiO_2 compact layers for low temperature ($T = -70$ °C) and the predictions of the model for the low diffusion coefficient considering $\tau_0 = 2$ ps and different a and b values.

calculated from the model for two different cases are also shown. Considering that the carriers are injected from the dye in a narrow region of the TiO_2, the values of a and b used in this simulation could be considered as the ranges of the experimental process, a between 0.2 and 0.3 nm and b between 0.6 and 1.4 nm.

The predictions of eq 8 have been compared with the results of integrating numerically eq 4, observing that the approximation introduced to obtain eq 8 produces a relative error in the slope value of 3% in the case of $a = 0.2$ nm and $b = 0.6$ nm and of 8% in the case of $a = 0.3$ nm and $b = 1.4$ nm.

3.2. High-Temperature Results. As the temperature increases, the SPV transients depart from the curve of decay at low temperature, which is determined by recombination only (Figure 3). This fact indicates that the electrons diffuse away from the injection region until they return also by diffusion to the high recombination region near the dye-covered surface, producing the fast decay observed at longer times. One expects that the larger the layer, the longer the PV remains high, and this is observed in the thickness dependence of the SPV spectra at $T = 80$ and 230 °C, Figures 4c and 4d. As remarked before, the role of diffusion is more clearly observed in thicker samples of 100 nm, Figure 5; however, these results will be analyzed in a separate work.

To model the high-temperature transients, the spatial distribution, $\Delta n(x,t)$, is obtained integrating the transport equation with tunneling recombination near the surface

$$\frac{\partial \Delta n}{\partial t} = D\frac{\partial^2 \Delta n}{\partial x^2} - \frac{\Delta n}{\tau_0}\, e^{-2x/a} \qquad (9)$$

where D is the diffusion coefficient, which is assumed constant. Equation 9 has been solved numerically by the method of finite differences considering blocking boundary conditions at both dye/TiO_2 and TiO_2/substrate interfaces ($(\partial n/\partial x)_{x=0,L} = 0$).

The assumption of diffusive transport has been checked self-consistently, comparing the drift and diffusion currents resulting from the electron distribution obtained by eq 9. Diffusion currents are generally much larger than drift currents; for example, in the case of a layer with $L = 20$ nm, $D = 10^{-5}$ cm^2/s, $\tau_0 = 2$ ps, $a = 0.25$ nm, and $b = 1$ nm, the drift current at $x = 2$ nm is 8.5×10^{-5} mA while the diffusion current is 24 mA, which justifies that the Coulomb interaction was neglected.

Figure 7 shows simulated SPV transients for varying thicknesses of the film. The normalization of SPV allows us to consider that the same amount of charge has been injected

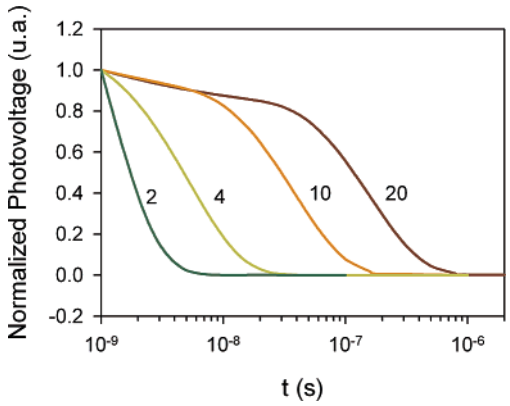

Figure 7. Photovoltage transient simulations, normalized to the value of photovoltage at $t = 1$ ns, for various layer thicknesses indicated in nanometers, $D = 10^{-5}$ cm^2 s^{-1}, $\tau = 2$ ps, and $a = 0.25$ nm. The injected distribution at $t = 0$ is an exponential function with $\Delta n(x = 0) = 1 \times 10^{16}$ cm^{-3} and $b = 1$ nm.

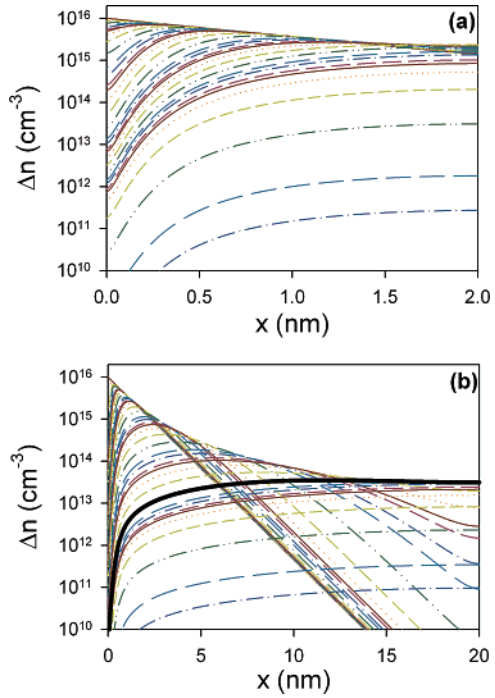

Figure 8. Snapshots of the evolution of excess electrons for $D = 10^{-5}$ cm^2 s^{-1}, $\tau = 2$ ps, and $a = 0.25$ nm. The injected distribution at $t = 0$ is an exponential function with $\Delta n(x = 0) = 1 \times 10^{16}$ cm^{-3} and $b = 1$ nm. (a) $L = 2$ nm. The times of electron distribution are logarithmically distributed from $t = 0$ to $t = 0.1$ μs. (b) $L = 20$ nm. The electron distribution is shown for different times separated logarithmically from $t = 0$ to $t = 1$ μs.

independently of the layer thickness. The progressive retardation of the decay of the PV at increasing layer thicknesses due to longer diffusion times is clearly observed in the simulation as well as in the measurement in Figures 4c and 4d. Therefore, the model presented explains qualitatively the general trends observed in the experimental measurements. As an illustration, Figure 8a shows the evolution of electron distribution in the thinnest layer considered (2 nm). Due to the small thickness, the charge separation by diffusion is strongly limited, producing a rapid SPV decay. Note the progressive extraction of the carriers nearest to the surface as implied by eq 1. Figure 8b shows the evolution of electron distribution for a layer with $L = 20$ nm. In this case, the decay due to recombination is partially compensated by the spatial charge separation induced by diffusion. Additionally, diffusion displaces electrons out of the region with high recombination probability near the dye/TiO_2 interface, resulting in the delay of SPV decay. This effect is progressively enhanced as the thickness of the layer and consequently charge separation increase. In this sense, charge separation is limited by the layer thickness; for the 20 nm layer, the maximum charge separation is obtained for $t = 50$ ns; the distribution at this time is emphasized with a thicker black line in Figure 8b. This time coincides with the time position of the shoulder observed in the SPV transient, Figure 7. After this time, the SPV signal exhibits a fast decay governed by the back diffusion of electrons into the region of high recombination probability.

Our results can be related with the minimum thickness needed to obtain V_{oc} in electrochemical cells observed by Zaban and co-workers.[13] Ultrathin TiO_2 layers in the few nanometer range are strongly affected by tunneling recombination, while in the thicker layers injected electrons escape by diffusion from the high recombination region, and their accumulation in the interior of the film produces the electrochemical photovoltage.

In principle, a further description of the SPV transients should be possible considering that a transit time for diffusion over a distance d corresponds to the time constant d^2/D. However, a complete analysis of the experimental decays including diffusion is more complex because the diffusion time constant is influenced by the removal of carriers. To obtain a complete quantitative description of the experimental decays, a more sophisticated model considering disorder both in electronic states involved in charge transfer, as typically found in TiO_2, and in the transport process is required. These effects will introduce a dispersion of time constants for recombination, extending the SPV decay to a wide number of decades. A physical study of these aspects is beyond the scope of the present report and will be presented in separate publications.

4. Conclusions

SPV transients of ultrathin compact TiO_2 layers of different thicknesses sensitized with the N3 dye have been investigated. The general trends of the experimental data are well-described, considering a simple model with ultrafast injection of electrons in a narrow region in the dye/TiO_2 interface, i.e., spatially dependent recombination, and diffusion. The diffusion process for thicker samples produces a delay of the SPV decay, due to the increasing charge separation and to the displacement of electrons out of the region with high recombination probability near the dye/TiO_2 interface. Our results provide a new tool for monitoring the dynamic processes of electrons in ultrathin films used in a variety of applications, such as nanoparticle coating.

Acknowledgment. The work was supported by the Ministerio de Educación y Ciencia of Spain under project MAT2004-05168 and Acción Integrada UJI-HMI. A.B. is grateful to Dr. H.-J. Muffler for introducing him the ILGAR technique and to Dr. Ch.-H. Fischer for giving him the opportunity to use the ILGAR lab of his group. The authors are grateful to Dr. W. Bohne, Dr. E. Strub, and Dr. J. Röhrich for the ERDA analysis of the samples and to Dr. F. Lenzmann for providing the compact TiO_2 layer.

References and Notes

(1) Bisquert, J.; Cahen, D.; Rühle, S.; Hodes, G.; Zaban, A. *J. Phys. Chem. B* **2003**, *108*, 8106.

(2) Nelson, J.; Haque, S. A.; Klug, D. R.; Durrant, J. R. *Phys. Rev. B* **2001**, *63*, 205321.

(3) Barzykin, A. V.; Tachiya, M. *J. Phys. Chem. B* **2002**, *106*, 4356.
(4) Kopidakis, N.; Benkstein, K. D.; van de Lagemaat, J.; Frank, A. J. *J. Phys. Chem. B* **2003**, *107*, 11307.
(5) Fabregat-Santiago, F.; Bisquert, J.; Garcia-Belmonte, G.; Boschloo, G.; Hagfeldt, A. *Sol. Energy Mater. Sol. Cells* **2005**, *87*, 117.
(6) Bisquert, J.; Zaban, A.; Greenshtein, M.; Mora-Seró, I. *J. Am. Chem. Soc.* **2004**, *126*, 13550.
(7) Bisquert, J.; Vikhrenko, V. S. *J. Phys. Chem. B* **2003**, *108*, 2313.
(8) Duzhko, V.; Timoshenko, V. Y.; Koch, F.; Dittrich, T. *Phys. Rev. B* **2001**, *64*, 75204.
(9) Dittrich, T.; Duzhko, V.; Koch, F.; Kytin, V.; Rappich, I. *Phys. Rev. B* **2002**, *65*, 155319.
(10) Kumara, G. R. R. A.; Tennakone, K.; Perera, V. P. S.; Konno, A.; Kaneko, S.; Okuya, M. *J. Phys. D: Appl. Phys.* **2001**, *34*, 868.
(11) Zaban, A.; Chen, S. G.; Chappel, S.; Gregg, B. A. *Chem. Commun.* **2000**, *22*, 2231.
(12) Palomares, E.; Clifford, J. N.; Haque, S. A.; Lutz, T.; Durrant, J. R. *J. Am. Chem. Soc.* **2003**, *125*, 475.
(13) Chappel, S.; Grinis, L.; Ofir, A.; Zaban, A. *J. Phys. Chem. B* **2005**, *109*, 1643.
(14) Kronik, L.; Shapira, Y. *Surf. Sci. Rep.* **1999**, *37*, 1.
(15) Johnson, E. O. *J. Appl. Phys.* **1957**, *28*, 1349.
(16) Dittrich, T. *Phys. Status Solidi A* **2004**, *201*, R69.
(17) Clifford, J. N.; Palomares, E.; Nazeeruddin, M. K.; Grätzel, M.; Nelson, J.; Li, X.; Long, N. J.; Durrant, J. R. *J. Am. Chem. Soc.* **2004**, *126*, 5225.
(18) Bär, M.; Muffler, H.-J.; Fischer, C.-H.; Lux-Steiner, M. C. *Sol. Energy Mater. Sol. Cells* **2001**, *67*, 113.
(19) Dittrich, T.; Muffler, H.-J.; Vogel, M.; Guminskaya, T.; Ogacho, A.; Belaidi, A.; Strub, E.; Bohne, W.; Röhrich, J.; Hilt, O.; Lux-Steiner, M. C. *Appl. Surf. Sci.* **2005**, *240*, 236.
(20) O'Regan, B.; Schwartz, D. T. *J. Appl. Phys.* **1996**, *80*, 4749.
(21) Queisser, H. J.; Theodorou, D. E. *Phys. Rev. B* **1986**, *33*, 4027.
(22) Tachiya, M.; Mozumber, A. *Chem. Phys. Lett.* **1975**, *34*, 77.
(23) Dittrich, T.; Mora-Seró, I.; Bisquert, J. Unpublished work, 2005.